Supplementary Information

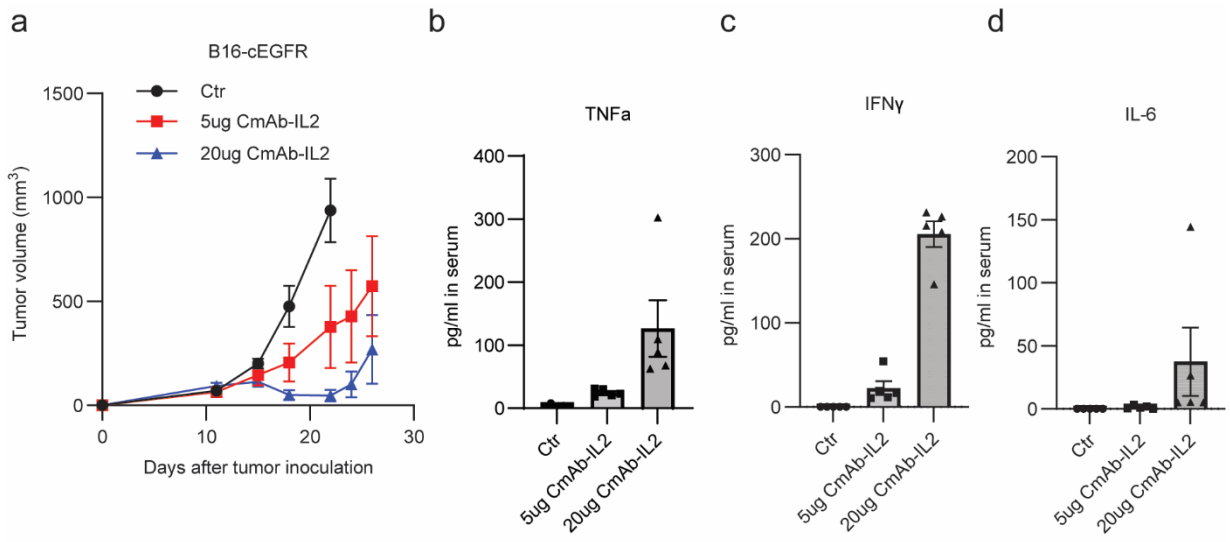

Supplementary Figure 1 (related to Figure 1). High-dose CmAb-IL2 (HD-CmAb-IL2) monotherapy has better antitumor efficacy but with side effects

(a-d) WT C57BL/6 mice (n=5/group) were injected subcutaneously with 4×10^5 B16-cEGFR cells, and treated i.p. with 5 μg or 20μg of CmAb-IL2 on days 11, 14, and 17. Tumor volumes were measured. The serum concentrations of TNF-α (b), IFN-γ (c) or IL-6 (d) were measured one day after the second treatment. Data are presented as mean ± SEM.

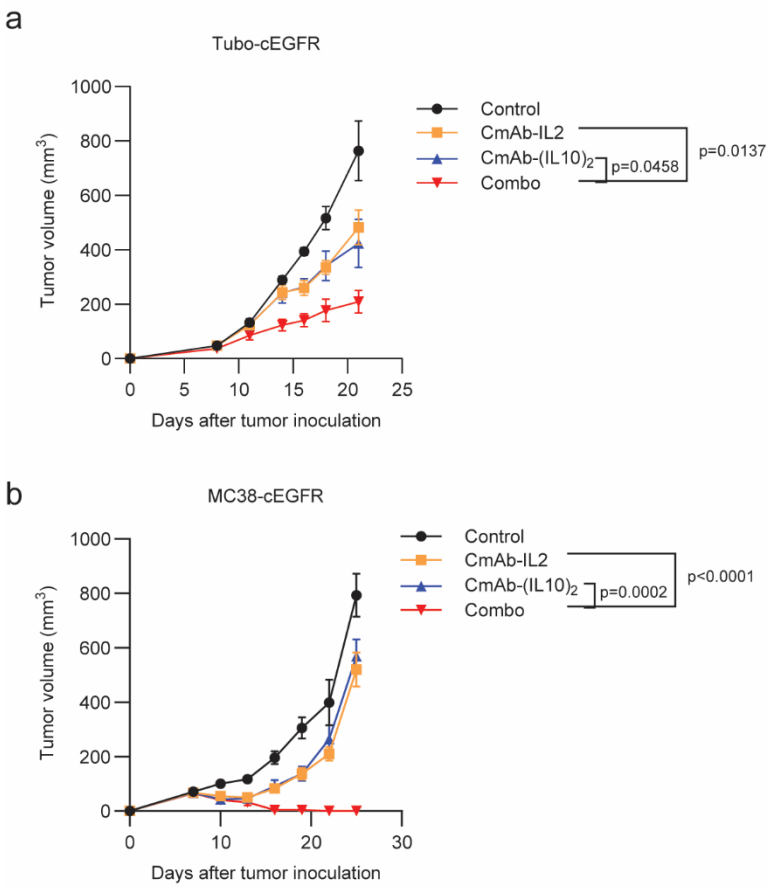

Supplementary Figure 2 (related to Figure 1). CmAb-(IL10)$_2$ combined with a well-tolerated dose of CmAb-IL2 significantly enhances antitumor efficacy compared to monotherapy

(a) WT BALB/c mice (n=4/group) were injected subcutaneously with 5×10^5 Tubo-cEGFR cells and were i.p. treated with 5 µg of CmAb-IL2, 80 µg of CmAb-(IL10)$_2$ or the combination on days 8, 11, and 14. Tumor volumes were measured, and the data are presented as mean ± SEM.

(b) WT C57BL/c mice (n=5/group) were injected subcutaneously with 1×10^6 MC38-cEGFR cells and were i.p. treated with 5 µg of CmAb-IL2, 80 µg of CmAb-(IL10)$_2$ or the combination on days 7 and 10. Tumor volumes were measured, and the data are presented as mean ± SEM.

Two-way ANOVA was used to analyze the tumor growth data.

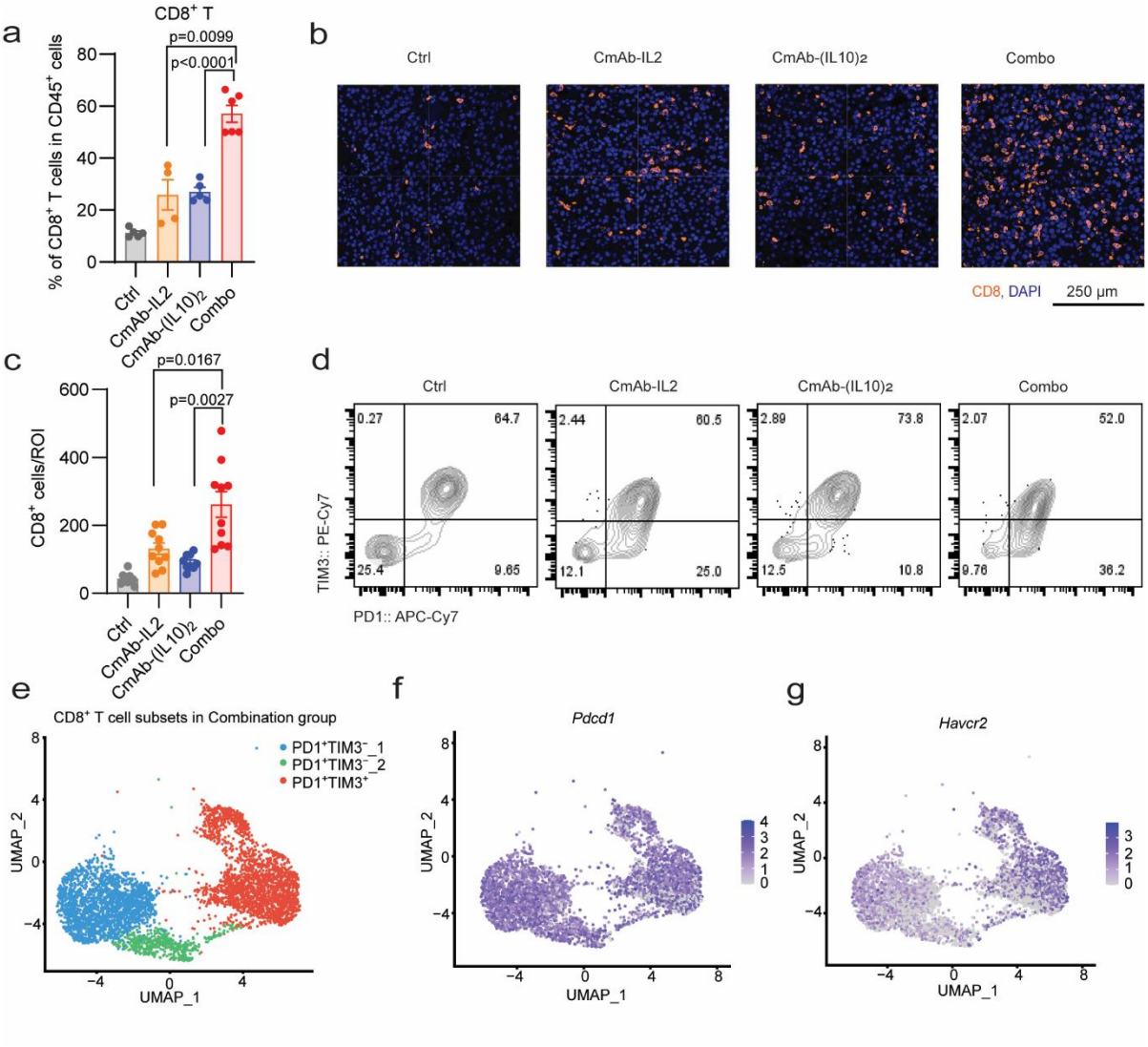

Supplementary Figure 3 (related to Figure 3). Combination of CmAb-(IL10)$_2$ with CmAb-IL2 therapy significantly increases CD8$^+$ T cells and modulates the phenotypic distribution of PD-1 and TIM-3 expression on T cells within tumors

(a-d) B16-cEGFR tumor-bearing WT C57BL/6J mice (Ctrl, n=5; CmAb-IL2, n=4; CmAb-(IL10)2, n=5; Combo, n=6) were treated with 80 μg of CmAb-(IL10)$_2$, 5 μg of CmAb-IL2 or the combination on days 9 and 12. The tumor tissues were harvested on day 14. (a) The frequency of CD8$^+$ T cells in tumor tissues was analyzed by flow cytometry. (b) Formalin-fixed paraffin-embedded (FFPE) sections (Thickness=5μm) were prepared for IHC staining; DAPI was used for nuclear staining, and representative images of immunohistochemical staining for CD8 (orange color) in consecutive sections of tumor tissues were presented. (c) The number of CD8$^+$ T cells in

each region of interest (ROI) was counted (c). The represented expression profiles of PD1 and TIM3 on $CD8^+$ T cells in each group were shown (d).

(e-g) Uniform manifold approximation and projection (UMAP) plot shows the clusters of tumor-infiltrating $CD8^+$ T cells from CmAb-$(IL10)_2$ and CmAb-IL2 combination treatment group (n=6) (e). The expression of *Pdcd1* (f) and *Havcr2* (g) in each cluster is shown.

Data in panels a and c are presented as mean ±SEM. Brown-Forsythe and Welch's ANOVA followed by Dunnett's T3 post-hoc test was used to analyze the data.

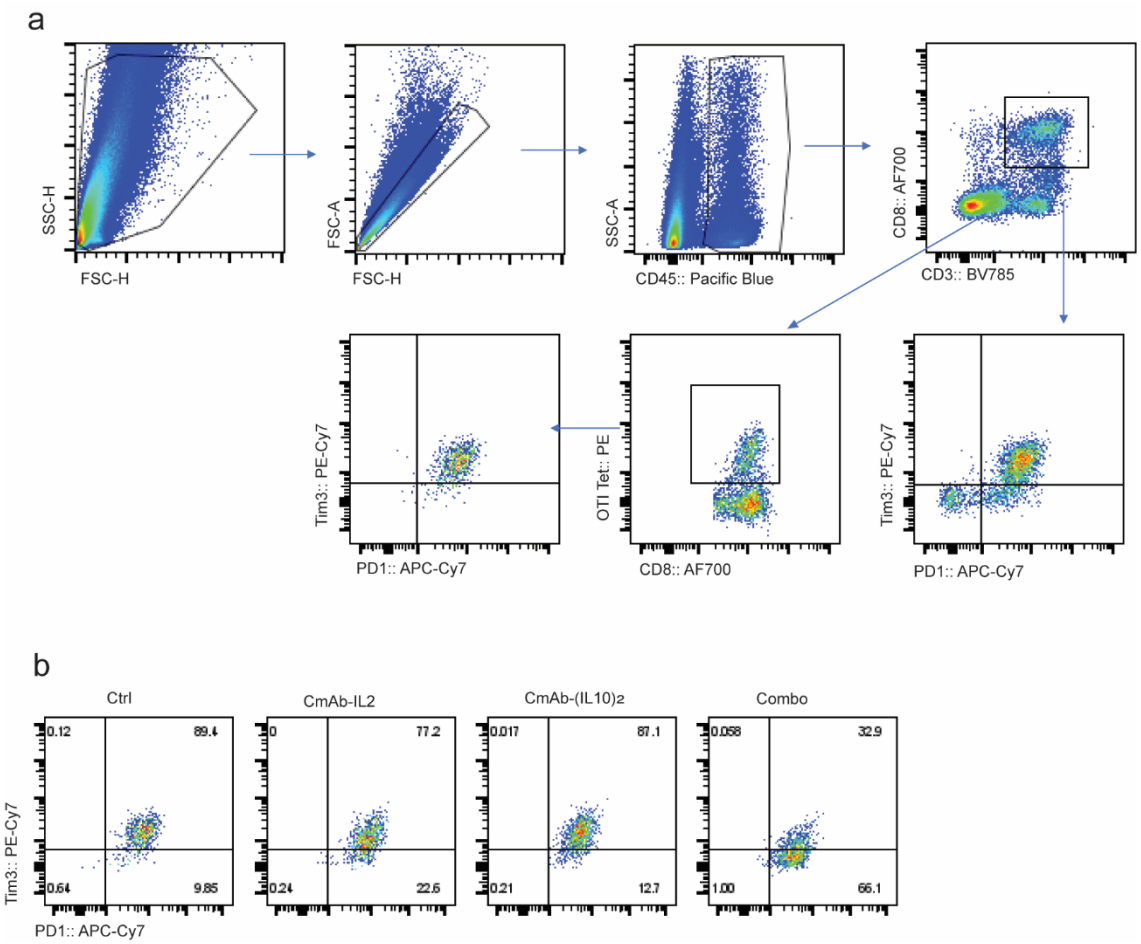

Supplementary Figure 4 (related to Figure 3). Combination of CmAb-(IL10)$_2$ with CmAb-IL2 therapy significantly increases less-exhausted, tumor-specific tetramer$^+$ CD8$^+$ T cells within tumors

WT C57BL/6J mice (Ctrl, n=5; other groups, n=4, as indicated in Figure 3i) were subcutaneously injected with 4×10^5 B16-cEGFR-OVA cells and treated i.p. with 80 μg of CmAb-(IL10)$_2$, 5 μg of CmAb-IL2 or the combination on days 9 and 12. Tumor tissues were harvested on day 14. The gating strategy is shown in (a). The frequency of PD1$^+$ TIM3$^-$ cells among Tetramer$^+$ OVA-specific CD8$^+$ T cells was analyzed by flow cytometry, with representative plots of the PD1 and TIM3 expression patterns shown in (b).

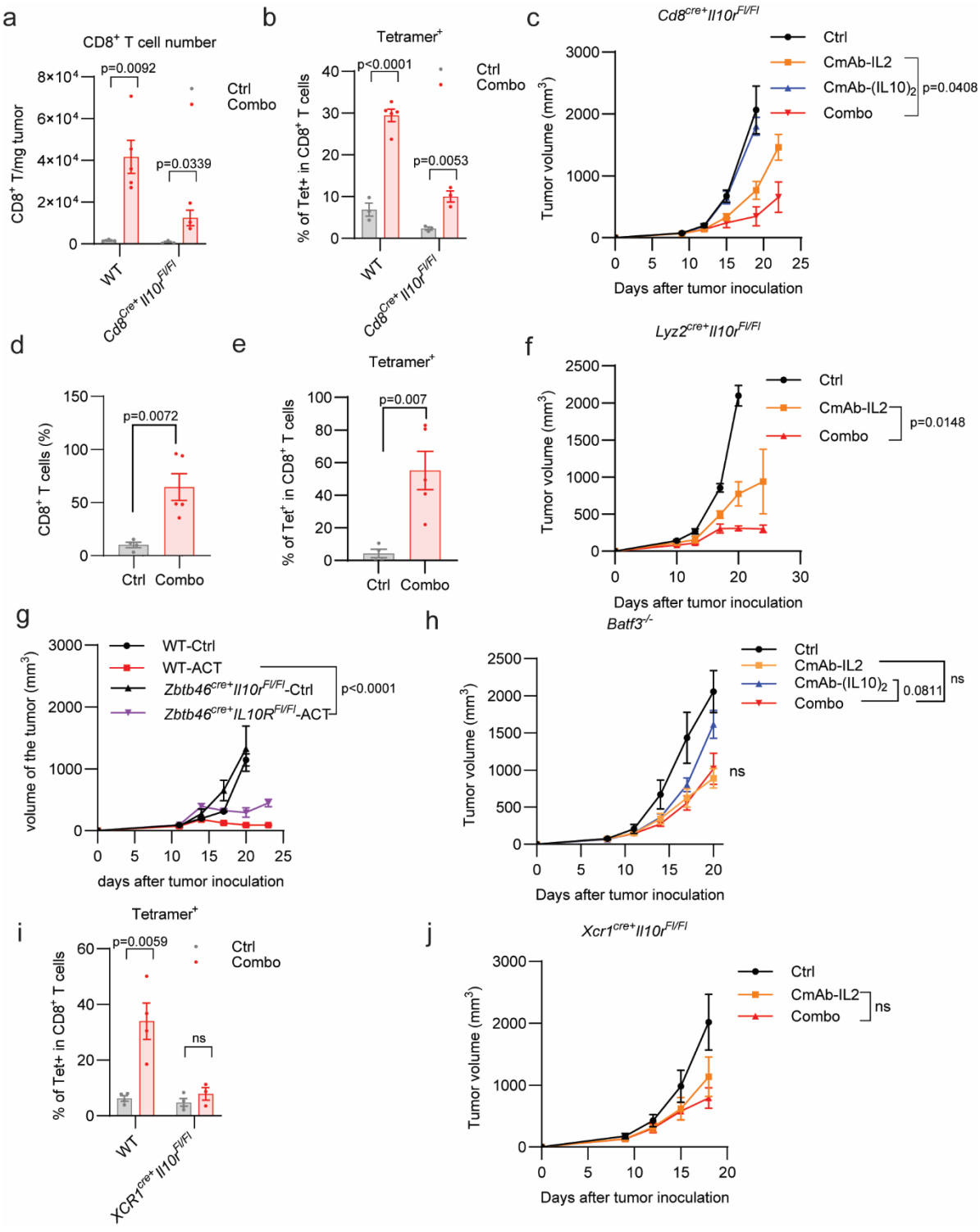

Supplementary Figure 5 (related to Figure 5). IL-10/IL10R axis in DCs, but not in T cells or macrophages, is critical for enhancing tumor-specific CD8$^+$ T cell response and therapeutic efficacy

(a-b) B16-cEGFR-OVA tumor-bearing WT (Ctrl, n=3; Combo, n=5) or *Cd8*$^{cre+/+}$-*Il10r*$^{Fl/Fl}$ C57BL/6J mice (n=3/group) received the same treatment regimen and underwent tumor collection as described in Fig 4a. The number of $CD8^+$ T cells in the tumor tissue (a), and the frequency of OVA-specific $CD8^+$ T cells (b) were analyzed by flow cytometry.

(c) B16-cEGFR tumor-bearing *Cd8*$^{cre+/+}$-*Il10r*$^{Fl/Fl}$ C57BL/6J mice (n=5/group) were treated i.p. with PBS, 5 μg of CmAb-IL2, 80 μg of CmAb-$(IL10)_2$ or the combination on days 9, 12, and 15. Tumor volumes were measured, and the data are presented as means ± SEM.

(d-e) B16-cEGFR-OVA tumor-bearing *Lyz2*$^{cre+}$-*IL10R*$^{Fl/Fl}$ C57BL/6J mice (Ctrl, n=4; Combo, n=5) received the same treatment regimen and underwent tumor collection as described in Fig 4a. The frequency of both $CD8^+$ T cells among total T cells (d) and OVA antigen- specific $CD8^+$ T cells within total $CD8^+$ T cells (e) in the tumor tissue were analyzed by flow cytometry.

(f) B16-cEGFR tumor-bearing *Lyz2*$^{cre+}$-*Il10r*$^{Fl/Fl}$ C57BL/6J mice (n=4/group) were treated i.p. by 5 μg of CmAb-IL2 with or without 80 μg of CmAb-$(IL10)_2$ on days 11, 14 and 17. Tumor volumes were measured, and the data are presented as means ± SEM.

(g) B16-cEGFR-OVA tumor-bearing WT (n=5/group) or *Zbtb46*$^{cre+}$*Il10r*$^{Fl/Fl}$ C57BL/6J mice (n=3/group) were i.v. treated with 1×10^6 pre-activated OT-1 $CD8^+$ T cells on days 11 and 14. Tumor volumes were measured, and the data are presented as means ± SEM.

(h) B16-cEGFR tumor-bearing *Batf3*$^{-/-}$ mice (n=6/group) were i.p. treated with 80 μg of CmAb-$(IL10)_2$, 5 μg of CmAb-IL2 or the combination on days 9, 12, and 15. Tumor volumes were measured twice weekly, and the data are presented as mean ± SEM.

(i) B16-cEGFR-OVA tumor-bearing WT C57BL/6J (n=4/group) and IL-10R knockout specially in cDC1 (*Xcr1*$^{cre+}$*Il10r*$^{Fl/Fl}$) mice (Ctrl, n=4; Combo, n=3) received the same treatment regimen and underwent tumor collection as described in Fig 4a. OVA antigen-specific $CD8^+$ T cells in tumors were detected by H-$2K^b$ OVA tetramer staining. The results were analyzed by flow cytometry, and the data are presented as mean ±SEM.

(j) B16-cEGFR tumor-bearing *Xcr1*$^{cre+}$*Il10r*$^{Fl/Fl}$ mice (Ctrl, n=5; CmAb-IL2, n=5; Combo, n=4) were treated i.p. with 80 μg of CmAb-$(IL10)_2$ and 5 μg of CmAb-IL2 combination therapy or 5 μg of CmAb-IL2 monotherapy on days 9, 12 and 15. Tumor volumes were measured twice weekly, and the data are presented as means ± SEM.

Two-way ANOVA was used to analyze tumor growth data; all other data were analyzed using unpaired *t*-tests.

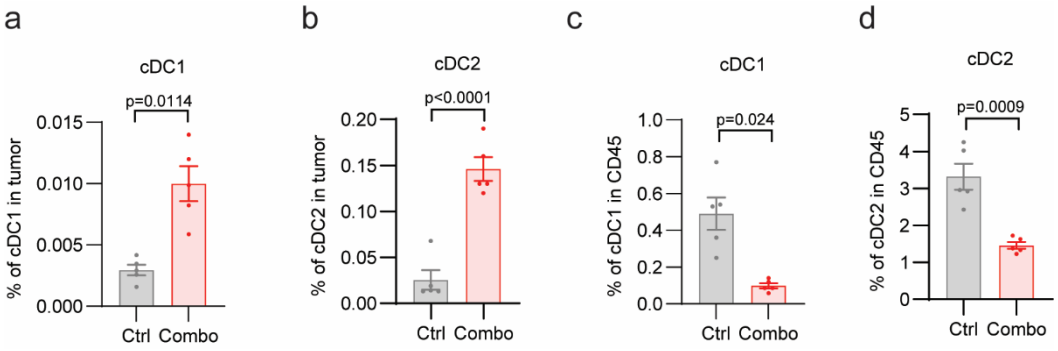

Supplementary Figure 6 (related to Figure 6). Combination of CmAb-(IL10)$_2$ with CmAb-IL2 therapy significantly increases DCs abundance despite a reduced relative frequency among CD45$^+$ cells within tumors

(a-d) WT C57BL/6J mice (n=5/group) were injected subcutaneously with 4×10^5 B16-cEGFR-OVA cells and i.p. treated with 80 µg of CmAb-(IL10)$_2$ and 5 µg of CmAb-IL2 on day 9 post tumor cell inoculation. Tumor tissues were harvested on day 12, and the frequency of cDC1 and cDC2 within the total tumor cell population (a, b) and among CD45$^+$ TILs (c, d) were quantified by flow cytometry. Data are presented as mean ±SEM. Unpaired t-tests were used to analyze the data.

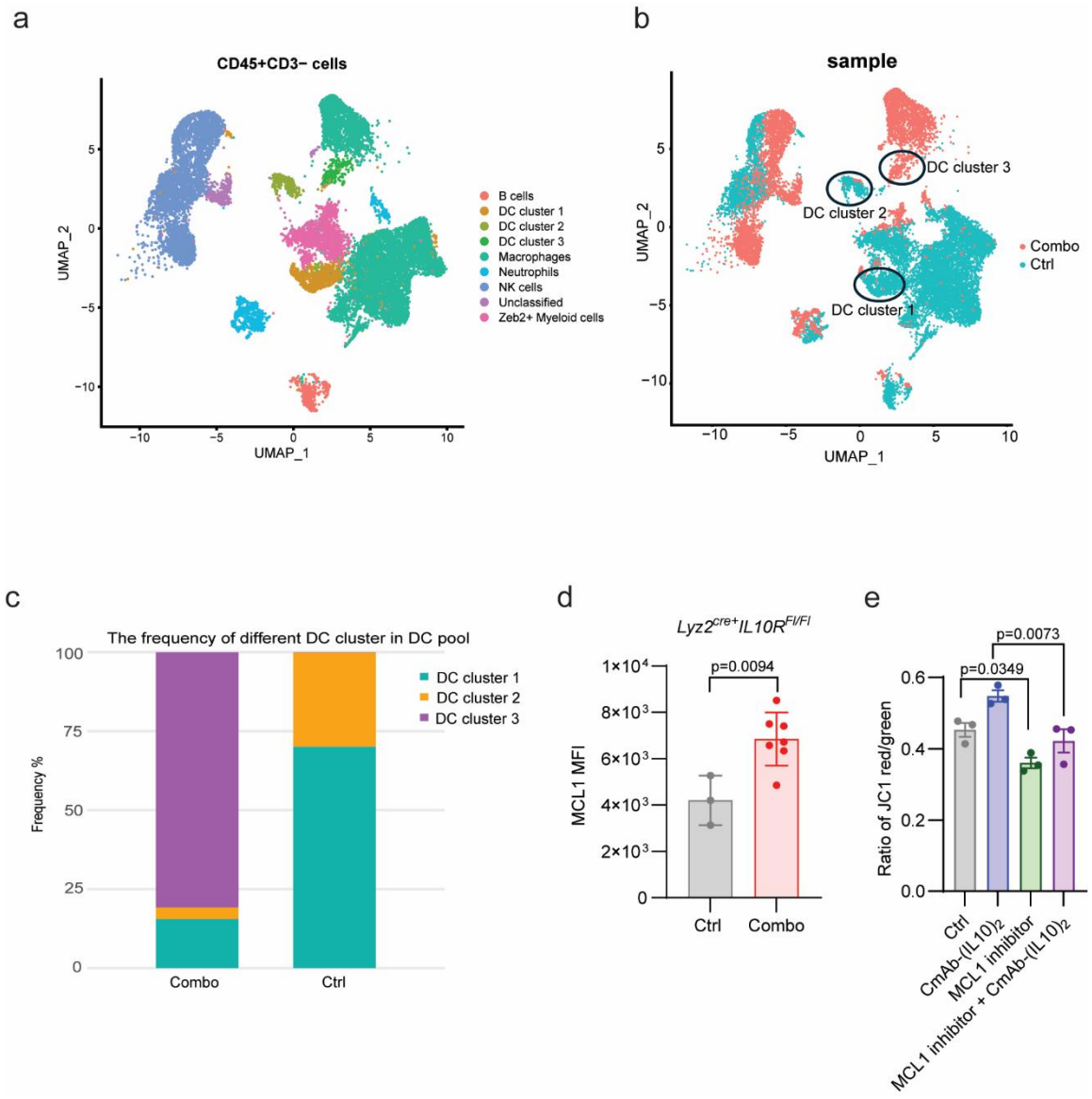

Supplementary Figure 7 (related to Figure 6). Combination of CmAb-(IL10)$_2$ with CmAb-IL2 therapy enriches clusters associated with enhanced DC function and health mitochondrial characteristics

(a-c) Uniform manifold approximation and projection (UMAP) analysis of tumor-infiltrating CD45$^+$ CD3$^-$ cells from control group (n=6) and the combination treatment group (CmAb-(IL10)$_2$ + CmAb-IL2) (n=6) identified three distinct DC clusters (a). The differential distribution of DC clusters between control and combination treatment group (b). The relative distribution of DC clusters within the DCs pool for both control and combination treatment group is shown (c).

(d) *Lyz2*$^{cre+}$*IL10*$^{Fl/Fl}$ mice were injected subcutaneously with 4×10^5 of B16-cEGFR-OVA cells, and i.p. treated with control (n=3) or the combination of 5 μg of CmAb-IL2 and 80 μg of CmAb-(IL10)$_2$ (n=7) on days 9 and 12. Tumor tissues were harvested on day 14, and the MCL-1

expression by DC cells was analyzed by flow cytometry. An unpaired *t*-test was used to analyze the data.

(e) DC cell line (JAWSII, n=3) was treated with the indicated reagents (CmAb-$(IL10)_2$ at 100ng/mL; MCL1 inhibitor at S63845 1uM) and stained with JC-1 (5 μM) for 3 hours. The ratio of intracellular red to green fluorescence of JC-1 was measured using Incucyte™. One-way ANOVA followed by Šídák's multiple comparisons test was used to analyze the data.

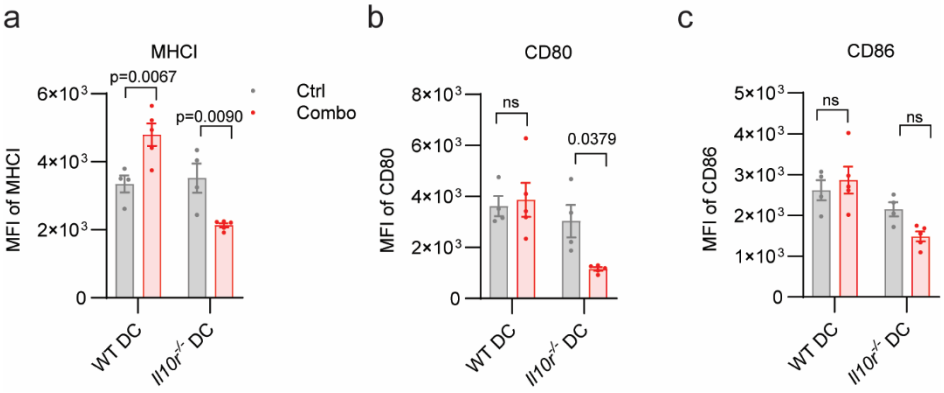

Supplementary Figure 8 (related to Figure 6). Combination therapy with CmAb-(IL10)$_2$ and CmAb-IL2 preserves intratumoral DC activity

(a-c) *Zbtb46*$^{cre+}$*Il10r*$^{Fl/Fl}$ mice (Ctrl, n=4; Combo, n=5) were injected subcutaneously with 4×10^5 B16-cEGFR-OVA cells. On day 9 post-tumor inoculation, tumor-bearing mice received an intratumoral injection of 2×10^6 BMDCs, consisting of a 1:1 mixture of WT (CD45.1$^+$) and *Il10r*$^{-/-}$ (CD45.2$^+$) DCs. On the same day, mice were also treated i.p. with 80 µg of CmAb-(IL10)$_2$ and 5 µg of CmAb-IL2. Tumor tissues were harvested on day 12, and the expression levels of MHC-I (a), CD80 (b) and CD86 (c) on transferred DCs were analyzed by flow cytometry. Data are presented as mean ±SEM. Two-way ANOVA followed by Šídák's multiple comparisons test was used to analyze the data.

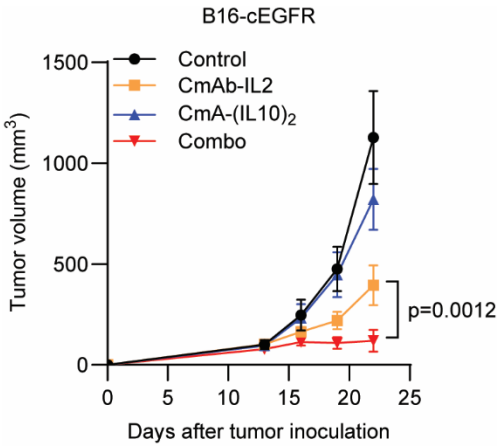

Supplementary Figure 9 (related to Figure 7). CmAb-(IL10)$_2$ combined with HD-CmAb-IL2 significantly enhances antitumor efficacy compared to monotherapy.

C57BL/6 mice (n=5/group) were subcutaneously injected with 4×10^5 B16-cEGFR cells, and i.p. treated with 20 μg of CmAb-IL2, 80 μg of CmAb-(IL10)$_2$ or the combination on days 13, 16, and 19. Tumor volumes were measured, and the data are presented as means ± SEM. Two-way ANOVA was used to analyze the tumor growth data.

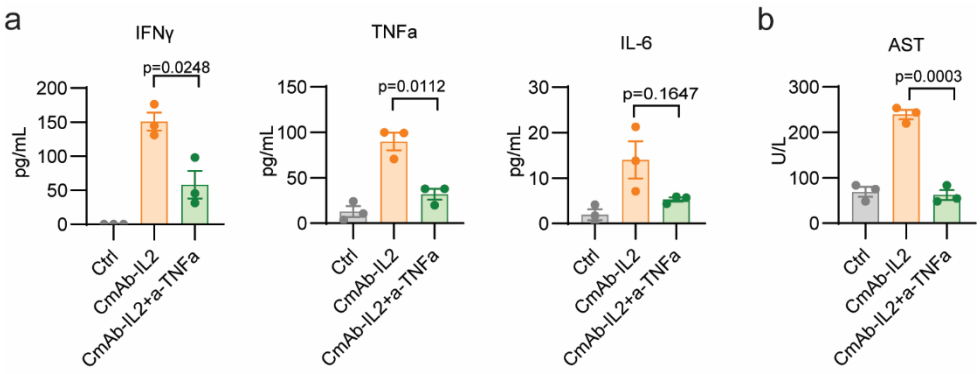

Supplementary Figure 10 (related to Figure 7). Systemic administration of anti-TNFα antibody mitigates toxicity associated with high-dose CmAb- IL2.

(a-b), WT C57BL/6 mice (n=3/group) were i.p. treated with PBS, or 20 µg of CmAb-IL2, with or without i.p. administration of a TNFα blocking antibody on days 0 and 2. Cytokine levels (a) and AST levels (b) were measured on day 4. Data are presented as mean ±SEM. Unpaired *t*-tests with Welch's correction were used to analyze the data in (a), and Brown-Forsythe and Welch's ANOVA followed by Dunnett's T3 post-hoc test was used to analyze the data in (b).

Supplementary Table 1. Key Resources Table

REAGENT or RESOURCE		SOURCE	IDENTIFIER
Antibodies	Dilutions		
*InVivo*MAb anti-mouse CD4 (GK1.5)	200ug/dose	BioXcell	Cat# BE0003-1
*InVivo*MAb anti-mouse CD8 (YTS 169.4)	200ug/dose	BioXcell	Cat# BE0117
*InVivo*MAb anti-mouse TNFα (XT3.11)	500ug/dose	BioXcell	Cat# BE0058
Pacific Blue™ anti-mouse CD45 Antibody	1:200	BioLegend	Cat# 103126
FITC anti-mouse CD45.2 Antibody	1:200	BioLegend	Cat# 109806
APC anti-mouse CD45.1 Antibody	1:200	BioLegend	Cat# 110714
Brilliant Violet 785™ anti-mouse CD3ε Antibody	1:200	BioLegend	Cat# 100355
Alexa Fluor® 700 anti-mouse CD8a Antibody	1:200	BioLegend	Cat# 100730
Brilliant Violet 605™ anti-mouse CD4 Antibody	1:200	BioLegend	Cat# 100548
APC/Cyanine7 anti-mouse CD279 (PD-1) Antibody	1:200	BioLegend	Cat# 135224
PE/Cyanine7 anti-mouse CD366 (TIM-3) Antibody	1:200	BioLegend	Cat# 119716
Anti-mouse IFN gamma Monoclonal Antibody (XMG1.2), APC	1:200	Thermo Fisher	Cat# 17-7311-82
FITC anti-human/mouse Granzyme B Recombinant Antibody	1:200	BioLegend	Cat# 372206
PerCP/Cyanine5.5 anti-mouse TNF-α Antibody	1:200	BioLegend	Cat# 506322
PE/Cyanine7 anti-mouse CD39 Antibody	1:200	Biolegend	Cat# 143806
APC/Cyanine7 anti-mouse CD11c Antibody	1:200	BioLegend	Cat# 117324
CD11c Monoclonal Antibody (N418), eFluor™ 506	1:200	Thermo Fisher	Cat# 69-0114-82
Brilliant Violet 605™ anti-mouse/rat XCR1 Antibody	1:200	BioLegend	Cat# 148222
PE/Cyanine7 anti-mouse CD172a (SIRPα) Antibody	1:200	BioLegend	Cat# 144008
PE/Cyanine7 anti-mouse/human CD11b Antibody	1:200	BioLegend	Cat# 101216
PerCP-Cy™5.5 Rat Anti-CD11b Antibody	1:200	BD Biosciences	Cat# 550993
Alexa Fluor® 700 anti-mouse I-A/I-E Antibody	1:200	BioLegend	Cat# 107622
Brilliant Violet 785™ anti-mouse F4/80 Antibody	1:200	BioLegend	Cat# 123141
PerCP/Cyanine5.5 anti-mouse CD40 Antibody	1:200	BioLegend	Cat# 124623
PE/Cyanine7 anti-mouse CD80 Antibody	1:200	BioLegend	Cat# 104734
FITC anti-mouse CD86 Antibody	1:200	BioLegend	Cat# 105110
MHC Class I (H-2Kb) Monoclonal Antibody (AF6-88.5.5.3), APC	1:400	Thermo Fisher	Cat# 17-5958-82
PE anti-mouse H-2Kb Antibody	1:400	BioLegend	Cat# 116508
MCL-1 Monoclonal Antibody (LVUBKM), PE	1:200	Thermo Fisher	Cat# 12-9047-41
Pacific Blue™ anti-human CD45 Antibody	1:200	BioLegend	Cat# 304022
PerCP/Cyanine5.5 anti-human CD3 Antibody	1:200	BioLegend	Cat# 300328
FITC anti-human CD8a Antibody	1:200	BioLegend	Cat# 300906
PE/Cyanine7 anti-human CD69 Antibody	1:200	BioLegend	Cat# 310912
APC anti-human CD11c Antibody	1:200	BioLegend	Cat# 301614
Brilliant Violet 785™ anti-human CD11b Antibody	1:200	BioLegend	Cat# 301346
iTAg Tetramer/PE - H-2 Kb OVA (SIINFEKL)	1:100	MBL	Cat# TB-5001-1
H-2 Kb (SIINFEKL), PE, 50 tests	1:100	immudex	Cat# JD02163-PE
Anti-FcγIII/II receptor (clone 2.4G2)	1:200	BD Biosciences	Cat# 553141
Anti-mouse CD8a (IHC, D4W2Z)	1:1000	Cell Signaling Technology	Cat# 98941
Chemicals, Peptides, and Recombinant Proteins			
FTY720 (hydrochloride)		Selleckchem	Cat# S5002

Fixable Viability Dye eFluor™ 506	Thermo Fisher	Cat# 65-0866-18
Fixable Viability Dye eFluor™ 780	Thermo Fisher	Cat# 65-0865-14
JC-1 Dye (Mitochondrial Membrane Potential Probe)	Thermo Fisher	Cat# MT3168
S63845	MedChemExpress	Cat# HY-100741
Brefeldin A Solution (1,000X)	BioLegend	Cat# 420601
eBioscience™ Cell Stimulation Cocktail (500X)	Thermo Fisher	Cat# 00-4970-93
$OVA_{257-264}$ (SIINFEKL)	Invivogen	Cat# vac-sin
RPMI-1640 Medium	Sigma- Aldrich	Cat# R8758
Dulbecco's Modified Eagle's Medium	Sigma- Aldrich	Cat# D6429
GE Healthcare Ficoll-Paque™ PLUS Media	Fisher	Cat# 45-001-750
Recombinant mouse GM-CSF	BioLegend	Cat# 576306
Critical Commercial Assays		
BD™ Cytometric Bead Array (CBA) Mouse Inflammation Kit	BD Biosciences	Cat# 552364
LEGENDplex™ Human Inflammation Panel 1 (13-plex)	BioLegend	Cat# 740809
BD™ Cytometric Bead Array (CBA) Mouse Th1/Th2 Kit	BD Biosciences	Cat# 551287
Opal Polaris 7 Color IHC Manual Detection Kit	Akoya Biosciences	Cat#NEL861001KT
True-Nuclear™ Transcription Factor Buffer Set	BioLegend	Cat# 424401
EasySep™ Mouse $CD8^+$ T Cell Isolation Kit	STEMCELL	Cat# 19853
EasySep™ Human CD34 Positive Selection Kit II	STEMCELL	Cat# 17856
EasySep™ Mouse T Cell Isolation Kit	STEMCELL	Cat# 19851
EasySep Biotin Positive Slection Kit II	STEMCELL	Cat# 17683
Experimental Models: Cell Lines		
B16	ATCC	Cat# CRL-6322
TUBO	Rovero, S., et al. 2000	N/A
MC38	Rosenberg, et al. 1986	N/A
FreeStyle™ 293-F	Thermo Fisher	Cat# R79007
A431	ATCC	Cat# CRL-1555
JAWSII	ATCC	Cat# CRL-3612
Experimental Models: Organisms/Strains		
C57BL/6J	Jackson Laboratory	Cat# 000664
BALB/cJ	Jackson Laboratory	Cat# 000651
B6.129S7-Rag1^{tm1Mom}/J	Jackson Laboratory	Cat# 002216
NOD.Cg-Prkdc^{scid} Il2rg^{tm1Wjl} Tg(CMV-IL3, CSF2, KITLG) 1Eav/MloySzJ	Jackson Laboratory	Cat# 013062
B6.129S(C)-Batf3^{tm1Kmm}/J	Jackson Laboratory	Cat# 013755
B6.129S2-*Il10rb*^{tm1Agt}/J	Jackson Laboratory	Cat# 005027
B6.129P2-*Il10*^{tm1Cgn}/J	Jackson Laboratory	Cat# 002251
B6(SJL)-*Il10ra*$^{tm1.1Tlg}$/J	Jackson Laboratory	Cat# 028146
B6.Cg-*Zbtb46*$^{tm3.1(cre)Mnz}$/J	Jackson Laboratory	Cat# 028538
C57BL/6-Tg(Cd8a-cre)1Itan/J	Jackson Laboratory	Cat# 008766
B6.129P2-*Lyz2*$^{tm1(cre)Ifo}$/J	Jackson Laboratory	Cat# 004781
B6(129S4)-*Xcr1*$^{tm1.1(cre)Kmm}$/J	Jackson Laboratory	Cat# 035435
B6.129S4-*Ifng*$^{tm3.1Lky}$/J	Jackson Laboratory	Cat# 017581
B6.SJL-*Ptprc*^{a} *Pepc*^{b}/BoyJ	Jackson Laboratory	Cat# 002014
C57BL/6-Tg(TcraTcrb)1100Mjb/J	Jackson Laboratory	Cat# 003831
Software and Algorithms		

GraphPad Prism software 7.0	GraphPad Software, Inc.	https://graphpad.com/scientific-software/prism/
Image Lab™ Software	Bio-Rad	http://www.bio-rad.com/en-us/category/image-analysis-software
CytExpert	Beckman Coulter, Inc	https://www.beckman.com/coulter-flow-cytometers/cytoflex/cytexpert
FlowJo	Tree Star Inc.	https://www.flowjo.com/solutions/flowjo
Incucyte	Sartorius	https://www.sartorius.com/en/products/live-cell-imaging-analysis/live-cell-analysis-software
QuPath		https://qupath.github.io/